Experimental identification and simulation of rotor damping

Lothar Gaul[1], André Schmidt[2]

University of Stuttgart, Institute of Applied and Experimental Mechanics, Pfaffenwaldring 9, 70550 Stuttgart, Germany
[1] e-mail: gaul@iam.uni-stuttgart.de
[2] e-mail: schmidt@iam.uni-stuttgart.de

ABSTRACT

The paper at hand shows how structural damping and stiffness parameters in shrunk joints can be determined by a generic joint experiment. With thin-layer elements these parameters from the joint experiment are coupled to the structures finite element model. Equivalent modal damping factors can be determined by performing a complex numerical modal analysis, by which the stability of the rotor can be tested. The two-disc rotor is examined as an application sample. This rotor consists of a shaft with two shrunk-on discs. With the above mentioned approach, and by considering structural damping added to material damping, the modal damping of the first torsional eigenfrequency is calculated and then compared to the results of an experimental modal analysis. The paper shows that the presented approach leads to a reliable approximation of the examined structure's dissipation properties. It serves as a prediction tool for the response behavior of a turbo-generator.

Keywords: Finite element method, damping, modal analysis, generic joint experiment, model of constant hysteresis

1 Introduction

For many applications damping is the major factor when stable operating states of a rotating machine are to be identified. In order to reliably predict if the operation state of a system is stable, dissipation properties have to be considered [1]. Predictive conclusions regarding stability therefore are only possible if the damping properties of a structure under consideration can be determined and then included into a numerical model as e.g. the FEM. Besides material damping, which can easily be determined from experiments or from literature, dissipation of a standardized joint is of particular importance. In metallic structures damping of joints usually outweighs material damping by one to two decades.

In order to quantitatively determine damping of joints, experimental testing needs to be developed by which properties of joints can be identified. Besides its dissipation properties also the tangential stiffness of the joint is relevant, since the structure is weakened by the joint which reduces eigenfrequencies compared to a solid connection. However, normal stiffness of joints only has minor influence on eigenfrequencies and -modes. Therefore it can simply be estimated or taken from experience. Alternatively the normal stiffness can also be determined by numerical contact analysis.

2 The two-disc rotor as a test structure

The examined structure consists of a shaft with two shrunk discs (see Figure 1) which will perform torsional vibrations. All pieces are made of steel. Measures such as material allowance in the contact area, surface roughness and press fit are common parameters used for turbine construction.

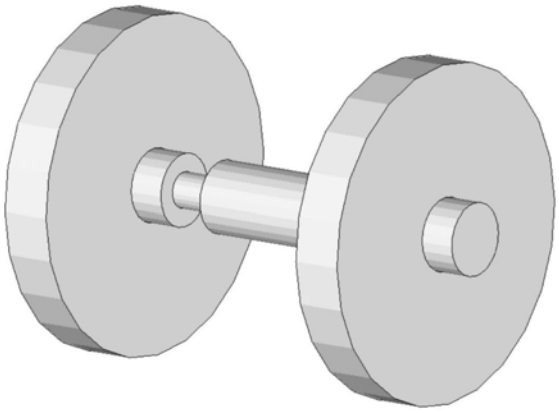

Fig. 1 3-D view of the two-disc rotor

A FE-analysis of the contact pressure with a press fit of 0.05 % contact overlap is shown in Figure 2. This results in an average contact pressure of 100 MPa; locally the pressure is as high as 150 MPa. This contact pressure corresponds to common values for rotating turbines. However, the two-disc rotor structure is examined without rotation and therefore shows the above mentioned contact pressure in a stationary state. A numerical modal analysis of the FE-model of the test structure shows that the torsional eigenfrequency is approximately 165 Hz.

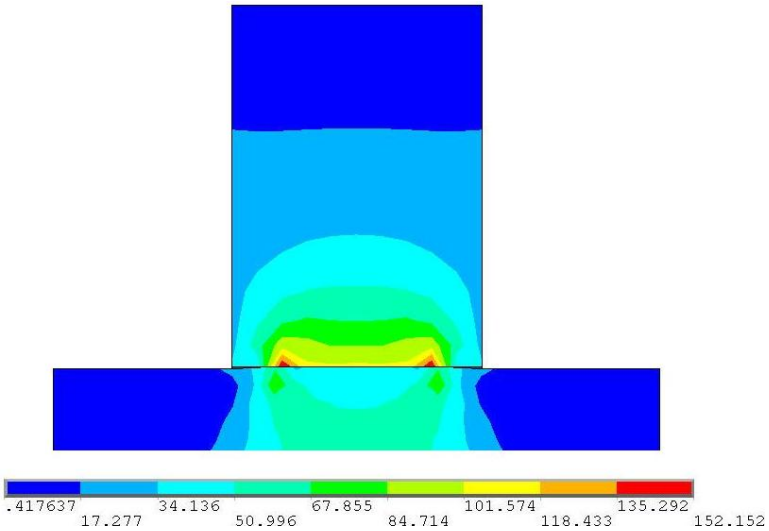

Fig. 2 Calculated contact pressure distribution between rotor and shrunk-on disc

3 Layout of the generic joint experiment

Since the contact parameters between rotor and discs are known in terms of surface roughness, contact pressure and frequency, a generic experiment can be conducted in order to determine the corresponding isolated joint's parameters. Figure 3 shows the measurement set-up. It consists of two small contact interfaces which are pressed against each other. The normal force in the joint is controlled by a bolt and measured by a force measurement ring. An excitation of the joint in the axial direction is realized by two masses on both sides of the joint where one mass is attached to a shaker. The mass shown on the right is connected to a leaf spring, such that the set-up is a two-mass resonator. When the resonance frequency is transmitted the axial force is increased considerably. On both sides of the joint two 3-dimensional accelerometers are placed. Their signals are used for the calculation of the relative displacement and therefore also for the stiffness of the joint and its dissipation behavior (see Section 4).

The boundary conditions for this generic experiment are known from the examination of the two-disc rotor: the experiment should be conducted with normal pressure of about 100 MPa and an excitation frequency nearby 165 Hz. The surface roughness also corresponds to the two-disc rotor.

The size of the contact interfaces measures 30 mm x 40 mm with a 14 mm diameter drilled hole in the middle. This results in a contact area of A = 1046 mm², for which a bolt force of 104.6 kN is needed. The amplitude of the axial force is defined by the input signal of the shaker.

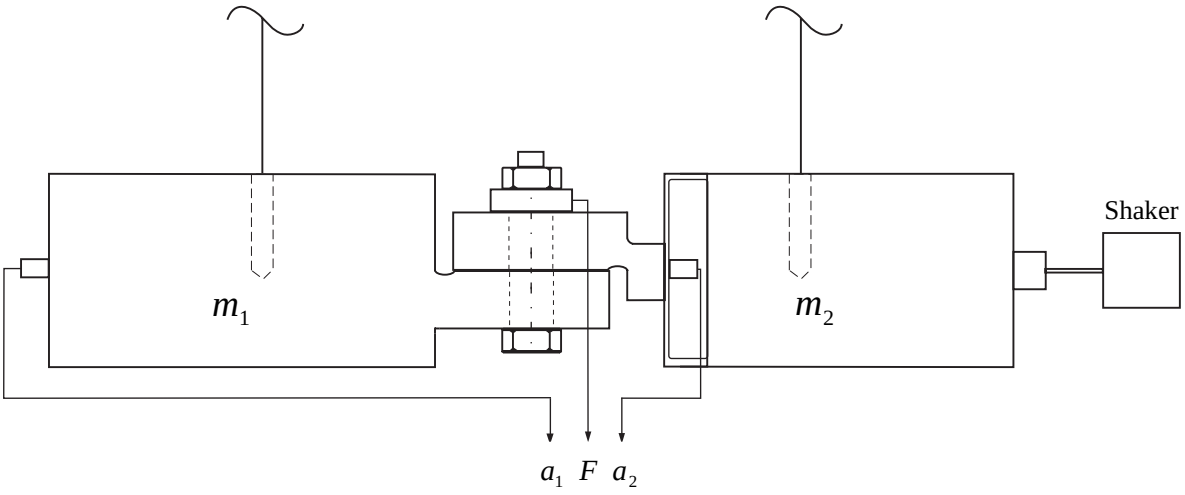

Fig. 3 Layout of the measurement set-up for determination of isolated joint's parameters

4 Determination of isolated joint's parameters

In order to determine stiffness and damping of the joint, the resonator is suspended by two thin wires attached to the masses at their centers of gravity. The excitation frequency of the shaker is 165 Hz. The relative displacement Δx is calculated by integrating the acceleration signals twice with respect to time

$$\Delta x(t) = \iint a_1(t)\,dt\,dt - \iint a_2(t)\,dt\,dt\,. \tag{1}$$

The tangential force F_T transmitted by the joint is obtained from the product of the free suspended mass m_1 and its acceleration a_1

$$F_\mathrm{T}(t) = m_1 a_1(t). \tag{2}$$

Using the results from these two time-dependent parameters, a hysteresis curve is determined (see Figure 4). The area of the hysteresis curve equals the energy W_d dissipated in one period. The ratio of the energy dissipated W_d divided by 2π times the maximum potential energy U_max gives the loss factor

$$\chi = \frac{W_d}{2\pi U_\mathrm{max}} \tag{3}$$

representing the damping in the examined joint. The slope of the hysteresis curve represents the tangential stiffness c of the joint

$$c = \frac{F_\mathrm{T}}{\Delta x}\,. \tag{4}$$

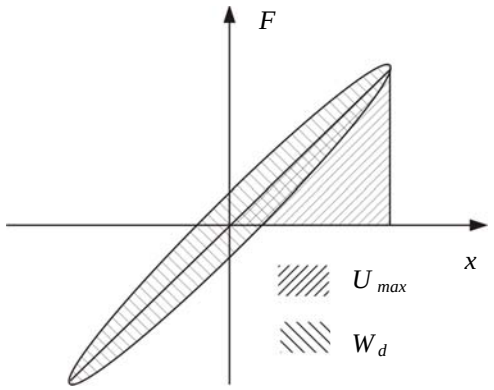

Fig. 4 Example of a hysteresis curve

Figure 5 shows several measured hysteresis curves recorded at different excitation amplitudes. The received signals are filtered in order to smoothen the curves. It can be seen that the joint's stiffness is nearly constant and the energy dissipation is small. This is due to the fact that with the chosen contact pressure and the excitation amplitudes only microslip occurs.

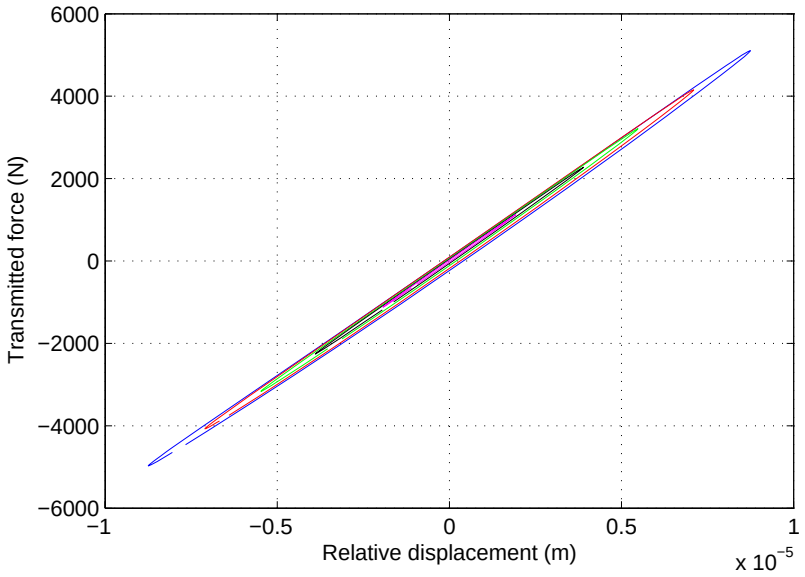

Fig. 5 Measured hysteresis curves

The experiment is carried out with different parameters in order to determine their influence on the parameters of the joint. In Figure 6 the influence of the contact pressure on the loss factor and the tangential stiffness are shown. The excited tangential force is between 2 kN and 6 kN. It can be seen that above a contact pressure of 20 MPa the parameters of the joint nearly stay the same. If the contact pressure is small only macro slip occurs and the measured loss factor increases significantly, while the contact stiffness collapses.

As shown in Figure 7 an increase of the excitation force results in a moderate change of the loss factor. However, it has to be taken into account that identifying the loss factor is related to some uncertainty. An influence of the excitation force on the tangential stiffness cannot be found (see Figure 5).

The influence of the surface finish is studied by changing its roughness R_z 16 to R_z 2 . However, a change of the joint's parameters cannot be found.

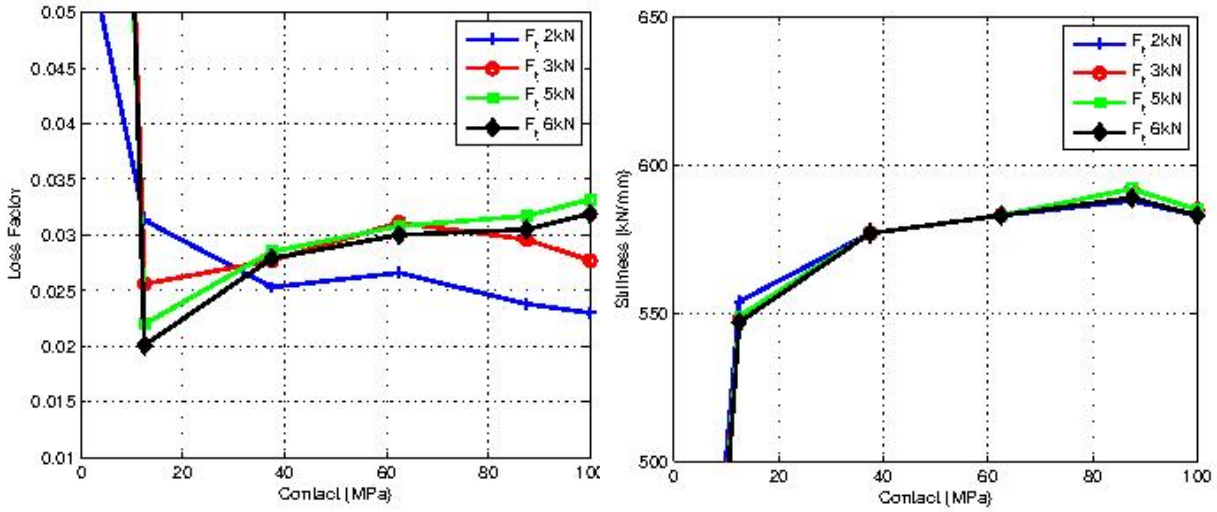

Fig. 6 Influence of contact pressure on loss factor and tangential stiffness

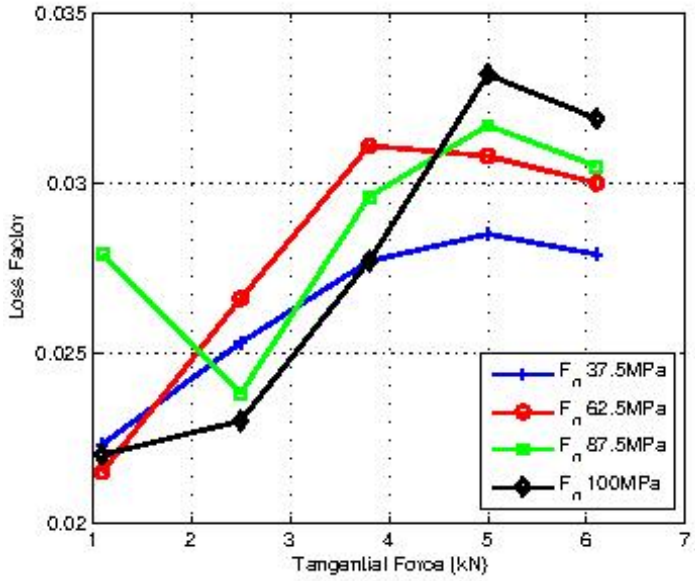

Fig. 7 Influence of tangential force on loss factor

In order to quantify the uncertainties of the measurements, the experiments are repeated a number of times with multiple reassemblies of the joint. Figure 8 shows exemplarily all measured results with variation of the excitation force. The result shows that the stiffness of the joint can be measured with high accuracy while the damping measurements contain a relatively high degree of uncertainty (± 30 %). The problem of precisely determining the energy dissipation in joints is also known in literature [12,13].

The average data determined by the joint measurements are:

$$\chi \approx 0.028 \qquad c \approx 580\ \text{kN/mm}. \tag{5}$$

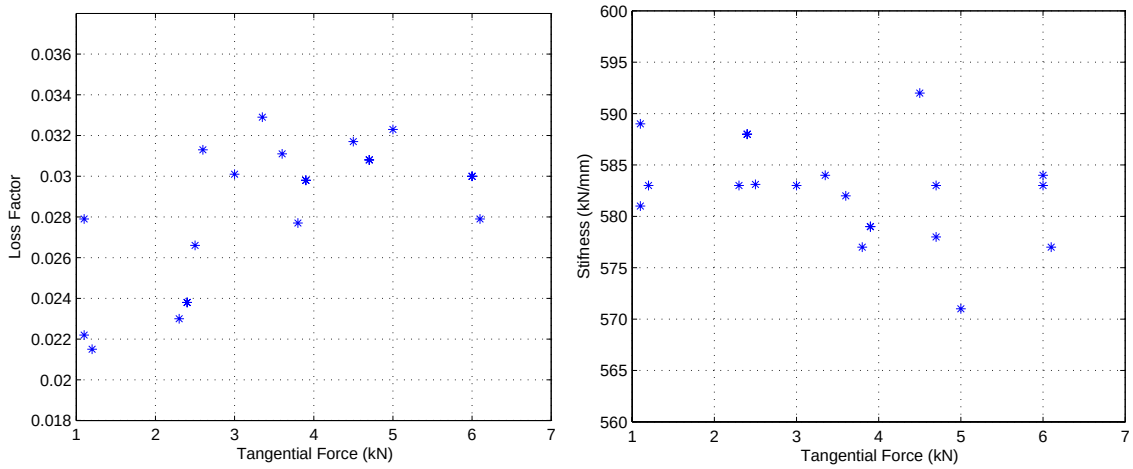

Fig. 8 Variation of loss factor (left) and tangential stiffness (right) measurements plotted versus different excitation levels

5 Two-disc rotor measurements

The experimental test set-up for measurements on the two-disc rotor is shown in Figure 9. The rotor is held by two cone-shaped supports in a lathe. This set-up minimizes the losses on the boundaries at the same time allowing torsional vibration of the rotor. A small cut-out at one disc allows for torsional excitation. Modal analysis with two accelerometers and impact excitation is performed. Later, additional measurements at the driving point are made.

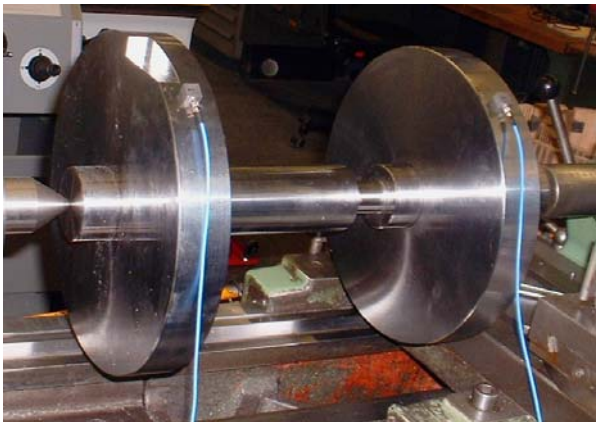

Fig. 9 Examined two-disc rotor with bearings and accelerometers

The FRF is shown in Figure 10. It can be seen that the torsional mode at 162 Hz is excited. The measurements are done with a block size of 28.800 points and a limit frequency of f_{max} = 1125 Hz. The measurement time per sample is 26 seconds. During the measurement time the acceleration signal decayed to noise level.

The amplitude decay measurement is shown in Figure 11. Three parameter identification methods are used to obtain damping and frequency of the torsional mode. At first, Me'Scope software is used to extract the damping from all measured data. Then, the measurements are transferred to MatLab and the damping is estimated by half-power method. Finally, an exponential function is curve-fitted to the amplitude decay measurements (Figure 11). The extracted modal damping factors ξ range from 0.024% to 0.029% of critical damping, with amplitude decay measurements showing a better consistency and a value of $\xi = 0.025\%$ [3].

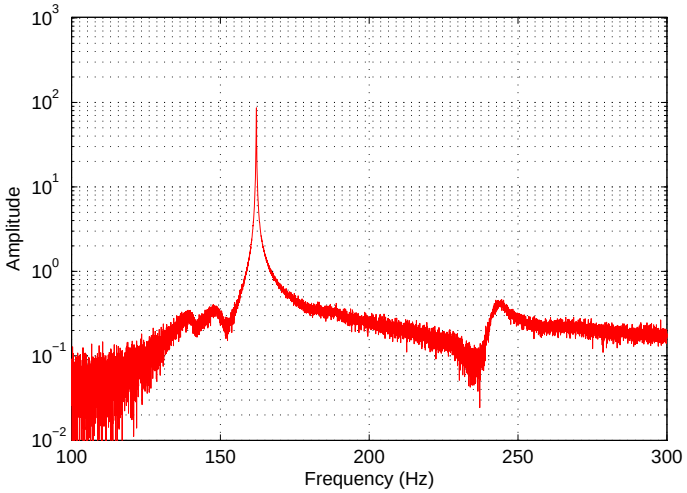

Fig. 10 Frequency Response Function (FRF) of the two-disk rotor

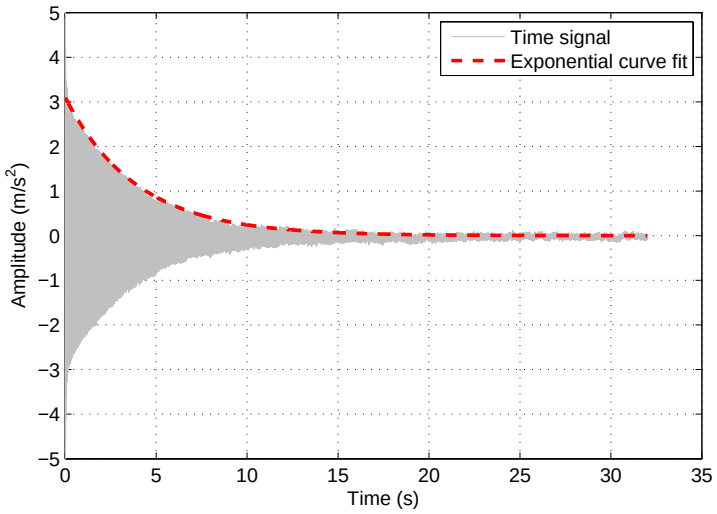

Fig. 11 Determining the damping factor by amplitude decay measurement

6 FE-modeling

It has been shown by experimental investigations that joint damping in metal structures is nearly frequency independent. Similar results have been shown for material damping in metals. Thus, for FE approach the model of constant hysteresis will be used. Such model makes sense only in frequency domain, while in time domain it might lead to non-casual material behavior [7]. The model of constant hysteresis of structural damping implies that damping is frequency independent.

Derivation of the FE equation of motion begins with an undamped system

$$\underline{M}\,\underline{\ddot{x}} + \underline{K}\,\underline{x} = \underline{0} \tag{6}$$

where $\underline{M}$ is a mass matrix, $\underline{K}$ is a real valued stiffness matrix, and $\underline{x}$ is the displacement vector. Eigenvalues and eigenmodes can be determined from a numerical modal analysis. Using the model of constant hysteresis, the damping in frequency domain will be incorporated by complex stiffness matrix $\underline{K}^*$ [1,3,6,7,10,14] with experimentally determined dissipation multipliers α_i and β_i for the material and the joint damping [4,9,11], respectively, and the associated elements stiffness matrices

$$\underline{K}^* = \underline{K} + j\sum_{i=1}^{n} \alpha_i \underline{K}_i^{(\text{material})} + j\sum_{i=1}^{m} \beta_i \underline{K}_i^{(\text{joint})}\,, \tag{7}$$

where n, m are the number of different materials and joints with different properties used in the model, respectively. The damping is low, implying $\alpha_i, \beta_i << 1$. The modified equation of motion (6), (7) can be solved for complex eigenvalues and eigenmodes with some commercial FE packages offering a complex solver, and in this case was performed with MSC.Nastran. The modal damping factors of the structure are read out from the solution file.

Thin-layer elements are used for the simulation of joints in the FE model [2]. The experimentally determined contact stiffness and dissipation parameters are used for constructing the stiffness matrices.
Thin-layer elements are normal hexahedral or pentahedral elements in which length or width to thickness ratio can be up to 1000: 1 without causing numerical problems during the calculation.

The stiffness of the generic joint (5) must be transferred into the FE model as a parameter of the thin-layer elements. A schematic of an arbitrary joint modeled by a thin layer is depicted in Figure 12. The force *F*, acting on both sides of the joint produces a shear stress τ in the layer. This stress can be expressed as

$$\tau = G\gamma \approx G\frac{u}{d}, \tag{8}$$

where G is the shear modulus and γ is the shear angle. The shear stress can also be calculated from the ratio of the applied tangential force *F* and the area of contact *A*

$$\tau = \frac{F}{A}. \tag{9}$$

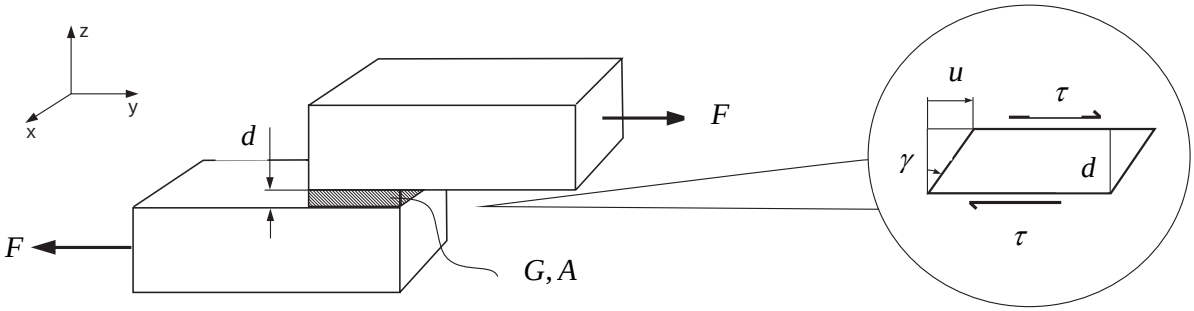

Fig. 12 Schematic of a joint with a thin-layer element

By combining both equations the force can be calculated as

$$F \approx \frac{GA}{d}u = c\,u. \tag{10}$$

The stiffness c in the equation is obtained from the generic joint experiment.

A basis for further examinations is that the joint shows orthotropic behavior, thus the thin-layer elements are modeled with respective material characteristics. Consequently the contact stiffness in normal and tangented direction may differ significantly. From Equation (10) the shear modulus can be approximated as

$$G = \frac{c\,d}{A}, \tag{11}$$

which depends linearly on the thickness *d* of the thin-layer elements.

Normal stiffness is not determined experimentally, but can be estimated from contact analysis. Physically sound limiting values for the selection of the normal stiffness are Youngs modulus of the surrounding material for the upper limit; for the lower limit isotropic joint behavior with disappearing transversal contraction $E = 2G$ can be used. The orthotropic matrix is defined as follows

$$\begin{bmatrix} \sigma_{xx} \\ \sigma_{yy} \\ \sigma_{zz} \\ \sigma_{xy} \\ \sigma_{yz} \\ \sigma_{zx} \end{bmatrix} = \begin{bmatrix} E_{11} & E_{12} & E_{13} & 0 & 0 & 0 \\ & E_{22} & E_{23} & 0 & 0 & 0 \\ & & E_{33} & 0 & 0 & 0 \\ & & & E_{44} & 0 & 0 \\ & & & & E_{55} & 0 \\ & & & & & E_{66} \end{bmatrix} \begin{bmatrix} \varepsilon_{xx} \\ \varepsilon_{yy} \\ \varepsilon_{zz} \\ \varepsilon_{xy} \\ \varepsilon_{yz} \\ \varepsilon_{zx} \end{bmatrix}. \tag{12}$$

The off-diagonal terms are zero for physical reasons (there is no transversal contraction generated by the contact interface). Also, since the interface has no stiffness in *x* and *y* direction (parallel to the joints surface), the terms E_{11} and E_{22} disappear. E_{33} represents the normal stiffness, whereas $E_{55} = E_{66} = G$ define the tangential stiffness of the joint. Since the joint exhibits no stiffness for in-plane shearing, E_{44} is also zero.

7 FE Simulation

The FE-model of the simulated two-disc rotor can be seen in Figure 13. It is modeled exclusively with isotropic hexahedral elements where the thin-layer elements have $d = 0.1$ mm thickness. In MSC.Nastran hysteretic damping can be defined by a material property card. In the FE calculation material damping is applied to all elements belonging to one of the three components of the structure, and joint damping is realized by application of damping to thin-layer elements. The parameters for the thin-layer elements are acquired from the generic joint experiment, while material damping was found in literature with a value of $\chi = 0.0001$[12]. For normal stiffness a value of $E_{33} = 80$ GPa is assumed, the result for the tangential direction is $E_{55} = E_{66} = 52$ MPa. Youngs modulus of steel is presumed with $E = 212$ GPa and Poisson's ratio $\nu = 0.3$.

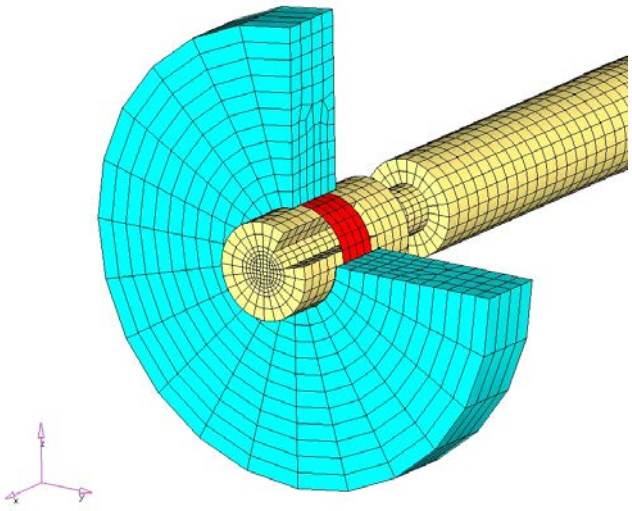

Fig. 13 FE-model of the examined two-disc rotor

With these values the torsional eigenfrequency is 160 Hz and the corresponding damping coefficient is $\chi = 0{,}00038$, converted to a modal damping factor $\xi = 0.019\%$.

A comparison of these values with the measured data (see Section 5) shows very good agreement. The difference in the eigenfrequency is only about 1%, the modal damping factor can be well estimated under the given uncertainties. The deviation is less than 25 %.

8 Summary

In this article a generic joint experiment is presented which enables an engineer to extract both, the tangential stiffness and the damping properties of a bolted joint connection. It turns out that the determination of damping properties of weakly damped structures, such as joints which only show microslip, goes along with substantial uncertainties. However, it succeeds to properly determine the dimension of damping. With this procedure at hand, a design engineer is enabled to make general statements about a structure's dynamic behavior before a prototype is being built and investigated.

As an example a two-disc rotor was investigated. The above mentioned approach was used to model the dynamic behavior of the structure with the FEM. The results of a numerical modal analysis were compared with the outcome of an experimental investigation by means of the first torsional eigenmode. It shows that the eigenfrequency can be calculated accurately, while the deviation of damping properties is in the range of 25%. Due to the difficulties of measuring small damping values the results are quite satisfactory.

Literatur

[1] Crandall, S.: The role of damping in vibration theory.*J. Sound and Vibration 11*, Nr. 1,pp. 3-18, 1970.

[2] Desai, C.S., Zaman, N.M., Lightner, J.G., Siriwardane, H.J.: Thin-Layer Element for Interfaces and Joints. *Int. J. Num. and Analyt. Meth. In geomechanics*, Vol. 8, pp. 19-43, 1984.

[3] Ewins, D.: Modal Testing: Theory Practice and Application .Second Edition, Research Studies Press.Baldock, 2000.

[4] Garibaldi, L., Onah, H. N.: *Viscoelastic Material Damping Technology*. BeccisOsiride. Torino, 1996.

[5] Gasch, R., Nordmann, R., Pfützner, H.: *Rotordynamik*, 2.Aufl. Springer-Verlag, Berlin Heidelberg, 2002.

[6] Gaul, L., Nitsche, R.: The role of friction in mechanical joints. *Applied Mechanics Reviews 54*, Nr. 2, pp. 93-106, 2001.

[7] Gaul, L., Bohlen, S., Kempfle, S.:Transient and Forced Oscillations of Systems with Constant Hysteretic Damping. *Mechanics Research Communications*,Vol.12(4), pp. 187-201, 1985.

[8] Gaul, L., Schmidt, A.,Bograd, S.: Experimentelle Ermittlung von Kennwerten zur Werkstoff- und Fügestellendämpfung sowie deren Berücksichtigung in Finite-Elemente-Berechnungen, Forschungsvereinigung Verbrennungskraftmaschinen (FVV), Heft 859, Frankfurt, 2008.

[9] Henwood, D. J.: Approximating the hysteretic damping matrix by a viscous matrix for modeling in the time domain, *J. Sound and Vibration 254*, Nr. 3, pp. 575-593, 2002.

[10] Inaudi, J. A., Makris, N.: Time-domain analysis of linear hysteretic damping, *Earthquake Enggr. And Structural Dynamics 25*, pp. 529-545, 1996.

[11] Lakes, R. S.: Viscoelastic Solids, CRC Press, Boca Raton, 1999.

[12] Nashif, A. D., Jones, D. I.G., Henderson, J.P.: *Vibration Damping*, John Wiley and Sons, New York, 1985.

[13] Ottl, D.: Schwingungen mechanischer Systeme mit Strukturdämpfung, VDI Verlag, Düsseldorf, (VDI-Forschungsheft Nr. 603), 1981.

[14] Schmidt, A., Gaul, L.: On the numerical evaluation of fractional derivates in multi-degree-of-freedom systems, *Signal Processing 86*, Nr. 10, pp. 2592-2601, 2006.